THE JOURNAL OF BIOLOGICAL CHEMISTRY VOL. 285, NO. 35, pp. 26933–26944, August 27, 2010

SOX9, through Interaction with Microphthalmia-associated Transcription Factor (MITF) and OTX2, Regulates *BEST1* Expression in the Retinal Pigment Epithelium*[S]

Received for publication, April 2, 2010, and in revised form, June 6, 2010 Published, JBC Papers in Press, June 8, 2010, DOI 10.1074/jbc.M110.130294

Tomohiro Masuda and Noriko Esumi[1]

From The Guerrieri Center for Genetic Engineering and Molecular Ophthalmology at The Wilmer Eye Institute and the Department of Ophthalmology, The Johns Hopkins University School of Medicine, Baltimore, Maryland 21287

***BEST1* is highly and preferentially expressed in the retinal pigment epithelium (RPE) and causes Best macular dystrophy when mutated. We previously demonstrated that the human *BEST1* upstream region −154 to +38 bp is sufficient to direct expression in the RPE of transgenic mice, and microphthalmia-associated transcription factor (MITF) and OTX2 regulate this *BEST1* promoter. However, a number of questions remained. Here, we show that yeast one-hybrid screen with bait corresponding to *BEST1* −120 to −88 bp identified the SOX-E factors, SOX8, SOX9, and SOX10. A paired SOX site was found in this bait, and mutation of either of the paired sites significantly decreased *BEST1* promoter activity in RPE primary cultures. Among the SOX-E genes, *SOX9* is highly and preferentially expressed in the RPE, and chromatin immunoprecipitation with fresh RPE cells revealed binding of SOX9, but not SOX10, to the *BEST1* region where the paired SOX site is located. *BEST1* promoter activity was increased by SOX9 overexpression and decreased by siRNA-mediated SOX9 knockdown. Importantly, SOX9 physically interacted with MITF and OTX2 and orchestrated synergistic activation of the *BEST1* promoter with the paired SOX site playing essential roles. A combination of the expression patterns of *SOX9*, *MITF*, and *OTX2* yielded tissue distribution remarkably similar to that of *BEST1*. Lastly, the *BEST1* promoter was also active in Sertoli cells of the testis in transgenic mice where SOX9 is highly expressed. These results define SOX9 as a key regulator of *BEST1* expression and demonstrate for the first time its functional role in the RPE.**

The retinal pigment epithelium (RPE)[2] has many specialized functions essential for vision and is indispensable for the survival and function of retinal photoreceptors (1, 2). RPE cells and melanocytes, two major pigmented cells in the body, share pigment-related genes such as tyrosinase (*Tyr*) and dopachrome tautomerase (*Dct*) and transcription factors regulating them such as microphthalmia-associated transcription factor (MITF); otherwise, these two cell types are distinct in many aspects. Although the molecular networks controlling gene expression in melanocytes have been extensively studied (3, 4), those in the RPE are still poorly understood. Among the key transcription factors required for RPE specification and development are MITF (3–9) and orthodenticle homeobox 2 (OTX2) (10–14). MITF and OTX2 proteins physically interact with each other and cooperatively activate some pigment-related genes in the RPE, such as *QNR71* and *Tyr* (15). Our previous studies found that human *BEST1*, a gene that is highly and preferentially expressed in the RPE but not related to pigment, is also regulated by MITF and OTX2 (16–18). However, a number of questions remained to be answered. Recently, it has been found unintentionally that SRY (sex-determining region Y) box 9 (SOX9) is robustly expressed in mouse RPE throughout embryonic development and into postnatal stages (19).

SOX9 is a member of the SOX family of transcription factors, which is characterized by the high mobility group domain, a DNA-binding motif of about 79 amino acids that is at least 50% identical to the high mobility group domain of SRY (20–22). SOX9 belongs to group E (SOX-E) along with SOX8 and SOX10 (20). SOX factors can act as architectural proteins that facilitate interaction between widely separated binding sites and promote the assembly of transcriptional complexes (21). SOX9 is essential for the development of several cell lineages, including Sertoli cells of the testis (23–26), chondrocytes (27, 28), pancreatic progenitors (29, 30), and oligodendrocytes in the spinal cord (31–33). In humans, heterozygous mutations in *SOX9* cause campomelic dysplasia (CD), a severe skeletal malformation syndrome frequently associated with XY sex reversal, and the majority of CD patients die during the neonatal period (34, 35). In mice, heterozygous *Sox9* knockouts ($Sox9^{+/-}$) recapitulate most of the skeletal abnormalities of CD and die perinatally (36). In the eye, SOX9 expression has been found in mouse retinal progenitor cells and Müller glia (19, 37),

* This work was supported, in whole or in part, by National Institutes of Health Grants EY015410, EY016398, and EY001765. This work was also supported in part by unrestricted funds from Research to Prevent Blindness, Inc. and generous gifts from Mr. and Mrs. Robert and Clarice Smith and the Guerrieri Family Foundation.

[S] The on-line version of this article (available at http://www.jbc.org) contains supplemental Figs. S1 and S2 and a table.

[1] To whom correspondence should be addressed: The Johns Hopkins University School of Medicine, Smith Bldg., Rm. 3041, 400 N. Broadway, Baltimore, MD 21287-9257. Tel.: 410-614-6110; Fax: 410-502-5382; E-mail: nesumi1@jhmi.edu.

[2] The abbreviations used are: RPE, retinal pigment epithelium; Tyr, tyrosinase; Dct, dopachrome tautomerase; MITF, microphthalmia-associated transcription factor; OTX, orthodenticle homeobox; BEST1, bestrophin 1; SOX, SRY (sex-determining region Y) box; CD, campomelic dysplasia; YOH, yeast one-hybrid; lacZ, β-D-galactosidase; CGGBP1, CGG triplet repeat-binding protein 1; GTF2IRD1, GTF2I repeat domain-containing 1; TK, thymidine kinase; qPCR, quantitative PCR; ChIP, chromatin immunoprecipitation; Col11a2, collagen type XI α2; Amh, anti-Müllerian hormone; Ptgds, prostaglandin D_2 synthase (brain); LEF1, lymphoid enhancer-binding factor 1; PGD_2, prostaglandin D_2.

and conditional knock-out mice revealed the essential role of SOX9 in the differentiation and/or survival of postnatal Müller glia (19). In matured human skin, SOX9 is a key player in ultraviolet B radiation-induced melanocyte differentiation and pigmentation by directly regulating *MITF* (38). SOX9 strongly binds as a dimer to a so-called "paired SOX site" that consists of two binding elements in opposite orientation with 3–4 bp spacing but can also bind to a single site as a monomer (39–46).

To understand the mechanisms regulating gene expression in the RPE, we have been analyzing the 5′-upstream region of *BEST1* as a model system (16–18). *BEST1* expression was initially found at the high level in the RPE with lower levels in the testis and brain (47); subsequently, it has also been found in specific cell types, such as airway epithelial cells (48) and hippocampal astrocytes (49). *BEST1* encodes bestrophin-1, a multispan transmembrane protein that seems to function as both a Ca^{2+}-activated chloride channel (50, 51) and a regulator of a voltage-gated Ca^{2+} channel (52–54). Mutations of *BEST1* cause Best disease (vitelliform macular dystrophy, VMD), an autosomal dominant, juvenile onset macular degeneration that is characterized by accumulation of lipofuscin-like material within and beneath the RPE and an abnormal electrooculogram (47). However, the phenotypic heterogeneity associated with *BEST1* mutations is increasingly complex with an additional four distinct ocular diseases described to date, *i.e.*, adult onset vitelliform macular dystrophy (AVMD) (55), autosomal dominant vitreoretinochoroidopathy (ADVIRC) (56), autosomal recessive bestrophinopathy (ARB) (57), and autosomal dominant and recessive retinitis pigmentosa (RP) (58). Furthermore, the mechanism by which mutations of *BEST1* cause Best disease has been controversial (50–54). Although Best disease was originally attributed to a loss of chloride channel activity, recent analyses of knock-in mice carrying the disease-causing mutation W93C in *Best1* suggested that Best disease likely results from dysfunction in the regulation of Ca^{2+} signaling (59).

Our previous studies using transgenic mice indicated that the human *BEST1* −154 to +38 bp region is sufficient to direct RPE-specific expression in the eye (16). Using *in vivo* electroporation, we further showed that the −154 to −104 bp segment contains regulatory elements contributing to a 10-fold increase in promoter activity in mouse RPE (60). In this study, we describe the identification of SOX9 by yeast one-hybrid screen as a factor that binds to this segment and plays a key role in the regulation of *BEST1* in the RPE. We show that SOX9 physically interacts with MITF and OTX2 and orchestrates synergistic activation of the *BEST1* promoter. Because the function of SOX9 in the RPE has never been recognized before, this is the first demonstration that SOX9 indeed plays a significant role in the regulation of a gene that is important for RPE physiology. We also suggest for the first time that *BEST1* is expressed in Sertoli cells of the testis in which SOX9 is highly expressed.

EXPERIMENTAL PROCEDURES

Plasmid Construction—A *BEST1* promoter-luciferase reporter construct containing the fragment −154 to +38 bp in pGL2-Basic vector (Promega, Madison, WI) was generated previously (*BEST1*−154/+38-luciferase) (18). Mutated *BEST1*−154/+38-luciferase constructs were made using PCR with synthetic long oligonucleotides containing mutations (underlined) in the paired SOX site, Site A (left, −107 to −101 bp, GACAAGG to GACGCGG, designated mutA), Site B (right, −96 to −90 bp, CTTTGTG to CGGCGTG, mutB), or both (mutAB) (Fig. 1*A*; also supplemental table). All fragments were ligated into SmaI site of pGL2-Basic and verified by sequencing. *BEST1*−154/+38-luciferase constructs containing mutation of E-boxes (m1, m2, and m1m2) and mutation of OTX sites (ma, mb, and mamb) were generated and described previously (16, 17). Expression vectors for human MITF-M and OTX2 were also generated previously (17, 18). Expression vectors for human SOX8, SOX9, and SOX10 were constructed using cDNAs generated by RT-PCR from RNAs that were extracted from testis, testis, and brain, respectively, with primer pairs containing restriction sites, an EcoRI site in forward primers and a HindIII site in reverse primers (supplemental table). Then, the cDNA fragments were inserted into EcoRI/HindIII sites downstream of the cytomegalovirus (CMV) promoter in pcDNA3.1/Myc-His(-) B vector (Invitrogen).

Yeast One-hybrid (YOH) Screen—A hybrid library of bovine RPE cDNAs fused to the activation domain of yeast transcription factor GAL4 in pGADT7 (Clontech) was constructed previously (16). Three yeast reporter vectors (pHISi, pHISi-1, and pLacZi) were made with a trimer of the *BEST1* −120 to −88 bp segment (designated Bait 6) using the Matchmaker One-Hybrid System (Clontech) (16). A 123-base sense strand oligonucleotide containing the trimer was entirely synthesized (supplemental table) and converted to double-stranded DNA, and the resultant DNA fragment was subcloned into each vector as described previously (16). Then, yeast strain YM4271 was transformed with these constructs, and a dual reporter strain containing both *HIS3* and *lacZ* constructs was generated (61). Using this dual reporter strain, YOH screen was performed as described previously (16, 61), and a total of $\sim 3 \times 10^6$ yeast colonies were screened.

YOH Assay—The yeast dual reporter strain containing Bait 6 was transformed with plasmid DNA purified from positive YOH clones for SOX8, SOX9, and SOX10. As control for bait, a yeast reporter strain containing Bait 11 (irrelevant to this study) was transformed in the same manner. As control for binding factors, plasmid DNA purified from yeast clones for CGGBP1 and GTF2IRD1, which were isolated by YOH screen with Baits 11 and 7, respectively, and empty pGADT7 were used. Growing colonies were streaked directly on nylon membranes on top of selection medium and stained by X-Gal.

Cell Culture—D407 human RPE and SK-MEL-5 human melanoma cell lines were cultured as described previously (16).

Pig RPE Primary Culture—Pig eyes obtained from a slaughterhouse were disinfected with 95% ethanol and dissected to remove cornea, lens, and retina. RPE/choroid eyecups were washed twice with phosphate-buffered saline (PBS) and filled with 0.25% trypsin and 1 mM EDTA up to ⅔ of the eyecups for digestion at 37 °C for 1 h. RPE cells were collected by gentle pipetting, transferred into Dulbecco's modified Eagle medium (DMEM) containing 20% fetal bovine serum (FBS) and 10 μg/ml gentamicin, and plated into a 60-mm dish per eye in the same medium. The culture medium was changed the next day (day 1) and day 4. By days 7–8, the cultures became confluent,

and then the culture medium was switched to DMEM containing 2% FBS. By 3–4 weeks, the cultures showed a cobblestone-like appearance. For transfection assays, RPE primary cells cultured for 4 weeks were treated with trypsin and seeded in 24-well plates at 2×10^5 cells/well in 500 μl of DMEM containing 2% FBS, and the next day transfection was carried out using Lipofectamine Plus (Invitrogen) for plasmid DNA and Lipofectamine 2000 (Invitrogen) for siRNA. The transfection efficiency for plasmid DNA checked by a plasmid containing the green fluorescent protein (GFP) gene was 10–20%. The transfection efficiency for siRNA checked by fluorescein-labeled double-stranded RNA oligonucleotide Block It (Invitrogen) was ~50%.

Transient Transfection—Transfection studies were carried out utilizing dual luciferase assays as described previously (16, 17). As host cells, D407, SK-MEL-5, and pig RPE primary cells were used to analyze basal promoter activity, and D407 cells were used for cotransfection. All plasmid transfections were performed using Lipofectamine Plus. For simple transfection with D407 and SK-MEL-5, plasmid DNA for each 35-mm dish included 1 μg of firefly luciferase vector and 0.1 ng of pRL-CMV containing *Renilla* luciferase gene (Promega) as control. For transfection with RPE primary cells, plasmid DNA for each well of 24-well plates included 0.4 μg of firefly luciferase vector and 0.05 ng of pRL-CMV. For cotransfection involving SOX9, because SOX9 activated the CMV promoter in pRL-CMV, pRL-TK containing *Renilla* luciferase gene driven by the TK promoter (Promega) was used as control. Also, because of high background activation of empty pGL2-Basic by a high dose of SOX9, 0.1 μg of SOX9 expression vector that did not activate pGL2-Basic was used throughout. Accordingly, for cotransfection with SOX9, plasmid DNA for each 35-mm dish included 1 μg of firefly luciferase vector, 0.1 μg of SOX9 expression vector, 0.4 μg of empty pcDNA3.1/Myc-His(-) vector, and 5 ng of pRL-TK. For cotransfection with various combinations of transcription factors, 0.1, 0.5, and 0.5 μg of expression vectors were used for SOX9, MITF, and OTX2, respectively, and the total amount of expression vectors was adjusted to 1.5 μg by adding pcDNA3.1/Myc-His(−). Accordingly, plasmid DNA for each 35-mm dish included 1 μg of firefly luciferase vector, 1.5 μg of expression vectors, and 5 ng of pRL-TK. As a firefly luciferase vector, *BEST1*−154/+38-luciferase constructs with wild-type sequence or mutation of the paired SOX site (mutA, mutB, or mutAB), E-boxes (m1, m2, or m1m2) (16), or OTX sites (ma, mb, or mamb) (17) were used. Transfections were performed three to five times in duplicate each time. Firefly luciferase activity was normalized by *Renilla* luciferase activity, and relative luciferase activity was calculated as the ratio of the normalized luciferase activity with *BEST1* promoter constructs to that with pGL2-Basic. To assess the effects of transcription factors, relative luciferase activity was calculated as the ratio of the normalized luciferase activity with the expression vectors to that with pcDNA3.1/Myc-His(−).

siRNA Transfection—Pig *SOX9* siRNAs 1, 2, and 3 (supplemental table) were made by a custom order (Dharmacon, Lafayette, CO) and transfected into 2×10^5 pig RPE primary cells/well in 24-well plates using 1 μl of Lipofectamine 2000. Based on pilot results, these siRNAs were used at 100 nM in all experiments. To check the efficiency of *SOX9* knockdown, total RNAs were extracted using an RNeasy mini kit (Qiagen, Valencia, CA) 36 h after transfection and analyzed by RT-qPCR with primers specific for pig *SOX9*, *SOX10*, and *GAPDH* (supplemental table). To analyze the effects of *SOX9* knockdown on *BEST1* promoter activity, sequential transfections were performed, first with siRNAs as described above and 24 h later with plasmid DNA including 0.4 μg of *BEST1*−154/+38-luciferase and 5 ng of pRL-TK using Lipofectamine Plus. Dual luciferase assays were performed 48–60 h after plasmid transfection, and results were normalized as described for transient transfection. Relative luciferase activity was calculated as the ratio of the normalized luciferase activity with siRNA to that without siRNA (presented as 1). With RPE primary cells derived from one pig eye, each siRNA was transfected in three wells, one for RNA and two for sequential transfections, and a total of eight independent primary cultures were used.

RT-qPCR—Total RNAs for expression studies were prepared previously from human RPE and retinal tissues as well as human culture cells, D407, ARPE19 RPE cell line, SK-MEL-5, and M1 RPE primary culture (16, 18). Total RNAs from 10 human tissues (liver, heart, brain, kidney, spleen, testis, thymus, bone marrow, colon, and small intestine) were purchased (Clontech). The expression levels of *SOX8*, *SOX9*, *SOX10*, *MITF*, *OTX2*, *BEST1*, and control *GAPDH* were analyzed by RT-qPCR with primers listed in the supplemental table as described previously (17). Based on threshold cycle (Ct) values, the expression level of each gene was normalized by that of *GAPDH* and presented as relative expression. To combine the expression patterns of multiple genes, relative expression in each sample (E_S: sample) was summed for all samples (E_T: total) for each gene. Then, E_S/E_T was calculated for each gene and multiplied by 10, and the resultant values for *SOX9*, *MITF*, and/or *OTX2* were multiplied for each sample.

Chromatin Immunoprecipitation (ChIP)—ChIP with fresh bovine RPE and retina was performed as described previously (16, 17, 62). Antibodies used were anti-SOX9 antibody AB5535 (Chemicon, Temecula, CA), anti-SOX10 antibody sc-17342 (Santa Cruz Biotechnology, Santa Cruz, CA), and anti-SOX10 antibody ab25978 (Abcam, Cambridge, UK). The final ChIP precipitates and diluted input (1:50) were analyzed by qPCR with primers at different locations of *BEST1* (supplemental table). Relative enrichment at each location was calculated as the ratio of the amount of PCR template in ChIP samples to that in diluted input. ChIP experiments were performed three times independently.

In Vitro Co-immunoprecipitation—Non-labeled and [^{35}S]methionine-labeled proteins for human SOX9, MITF-M, OTX2, and control luciferase were generated using the TnT T7 Quick Coupled Transcription-Translation System (Promega). A combination of proteins (indicated by + in Fig. 4), 15 μl of each non-labeled and ^{35}S-labeled, were mixed in 100 μl of PBS containing 0.01% IGEPAL CA-630 at room temperature for 2 h to form a protein complex; incubated with 1 μg of anti-SOX9 (AB5535), anti-MITF (C5 and D5, Lab Vision, Fremont, CA), or anti-OTX2 (ab21990, Abcam) antibody at 4 °C for 2 h; and precipitated with 50 μl of Protein A-Sepharose (GE Healthcare) at 4 °C for 3 h. After washing five times, bound proteins were

eluted as described previously (17). Samples were resolved by SDS-polyacrylamide gel electrophoresis (SDS-PAGE) and visualized with x-ray film after treating with Amplify (GE Healthcare). To check the input proteins, 1 μl of ^{35}S-labeled proteins was also analyzed.

Transgenic Mice, X-Gal Staining, and Immunohistochemistry—Transgenic mice carrying a *lacZ* reporter driven by the *BEST1* −424 to +38 bp promoter were generated previously (18). Although these transgenic lines were lost, we had kept frozen tissues mounted in OCT medium without fixation. Testis sections were cut at 10 μm on a cryostat for histological analyses. For staining with X-Gal, the sections were fixed in 0.5% glutaraldehyde in PBS at room temperature for 10 min and stained at 37 °C for 18 h as described previously (18). For immunohistochemistry, the sections were fixed in 1% paraformaldehyde in PBS at room temperature for 10 min followed by preincubation in 10% horse serum in PBS containing 0.2% Triton X-100 (PBST). Then, the sections were incubated with the anti-SOX9 antibody AB5535 at 1:200 dilution in 3% horse serum in PBST at 4 °C overnight, and the SOX9 antibody was detected with Alexa Fluor 488-conjugated anti-rabbit IgG antibody at 1:500 dilution (Invitrogen). The sections were mounted in VECTASHIELD mounting medium with DAPI (Vector Laboratories, Burlingame, CA), and images were taken on a scanning confocal microscope.

Statistical Analysis—Unpaired *t* test was used for statistical analysis.

RESULTS

YOH Screen with BEST1 Promoter Elements Identified SOX-E Factors—Our previous studies suggested that regulatory elements necessary for expression in mouse RPE exist in the *BEST1* −154 to −104 bp region (60). To identify factors that bind to this region by the YOH system, we designed three baits that were partially overlapped at both ends and collectively covered the entire region. Bait corresponding to the most proximal region was a trimer of the −120 to −88 bp segment and designated Bait 6. YOH screen of a hybrid library of bovine RPE cDNAs with Bait 6 yielded a total of 28 clones, and eight, five, and two clones encoded SOX9, SOX8, and SOX10, respectively. To test the sequence specificity of binding of these SOX-E factors, YOH-based binding assays were carried out. Growing colonies were streaked and stained by X-Gal to detect yeast cells turning blue in which a fusion protein binds to bait sequence. As expected, the three SOX-E factors bound to Bait 6 but not to irrelevant Bait 11, whereas CGGBP1 that was isolated by YOH screen with Bait 11 bound to it but not to Bait 6 (supplemental Fig. S1). In contrast, neither irrelevant factor GTF2IRD1 nor empty pGADT7 led to lacZ expression, confirming that the binding of the SOX-E factors was sequence-specific.

Paired SOX Site Contributes to BEST1 Promoter Activity—Of the three SOX-E factors, it was reported that SOX9 is expressed in mouse RPE from embryonic stages through adults (19), raising the possibility that SOX9 might be the regulator of *BEST1* in the RPE. Based on the reported findings that SOX9 regulates mouse *Col11a2* and *Ptgds* through paired SOX sites (underlined) CACAAGGCGTGCTTTGTC in the enhancer (41) and CACAAATGGTGCTTTGTG in the promoter (46), respectively, we reanalyzed the sequence of Bait 6. A similar paired site GACAAGGACTCCTTTGTG (Site A, left, −107 to −101 bp; Site B, right, −96 to −90 bp) was found with Sites A and B in an opposite direction and separated by 4 bases, and Site B was identical to the right site in the mouse *Ptgds* promoter (Fig. 1*A*). This *BEST1* paired SOX site is completely conserved between human and bovine. To test the functional importance of this paired SOX site, we analyzed the effect of its mutation on *BEST1* promoter activity by transient transfection using host cells with different expression profiles of the SOX-E genes. *BEST1* promoter-luciferase constructs were generated with wild-type sequence or mutation of Site A (designated mutA), Site B (mutB), or both (mutAB) in the context of the *BEST1* −154 to +38 bp fragment (*BEST1*−154/+38) (Fig. 1*A*). As expected, in D407 human RPE cells that express none of the SOX-E genes, mutA, mutB, or mutAB showed no effect on *BEST1* promoter activity (Fig. 1*B*). To the contrary, in SK-MEL-5 human melanoma cells that highly express *SOX10* but not other SOX-E genes, mutA, mutB, and mutAB all similarly and dramatically decreased *BEST1* promoter activity down to less than 1% of that of the wild-type construct ($p = 0.003$) (Fig. 1*B*). As host cells that more closely mimic *in vivo* RPE, we used pig RPE primary cells that still expressed *SOX9* and *SOX10* at 50–100 and 10–20%, respectively, of the levels in freshly harvested RPE cells at the time of luciferase assays (data not shown). In these RPE primary cells, mutA, mutB, and mutAB all significantly decreased *BEST1* promoter activity down to 28% ($p = 0.004$), 26% ($p = 0.0063$), and 27% ($p = 0.0027$), respectively (Fig. 1*B*). These differences in the effects of the mutated paired SOX site among the host cells are most likely due to the differential expression of the SOX-E factors and their interacting proteins. Interestingly, the residual activity of the mutated constructs in SK-MEL-5 cells was similar to the activity in D407 cells. These results indicate that the paired SOX site in the *BEST1* promoter is functional in cells expressing the SOX-E factors, and Sites A and B are equally important for its function.

SOX9 Is Highly and Preferentially Expressed in RPE—Expression is one of the key factors that determine which genes are biologically relevant in a specific cell type among members of the same protein family. Therefore, we analyzed the expression of *SOX8*, *SOX9*, and *SOX10* in various human tissues, including RPE and retina, by RT-qPCR together with samples from culture cells, D407, ARPE19 human RPE cell line, SK-MEL-5, and M1 human RPE primary culture. The expression patterns of the SOX-E genes were tissue-restricted with *SOX8* expressed preferentially in the testis, *SOX9* expressed preferentially in the testis and RPE, and *SOX10* expressed preferentially in the brain and RPE (supplemental Fig. S2). None of the SOX-E genes were significantly expressed in the cell lines except for *SOX10*, which was highly expressed in SK-MEL-5 as predicted from its importance in the melanocyte lineage. Although *SOX10* was also detected at a significant level in the RPE, we could not exclude the possibility that RPE RNA samples were contaminated with choroidal melanocyte RNA during extraction. However, because *SOX10* was also detected in M1 RPE primary culture even after a few passages, we assumed that *SOX10* is likely

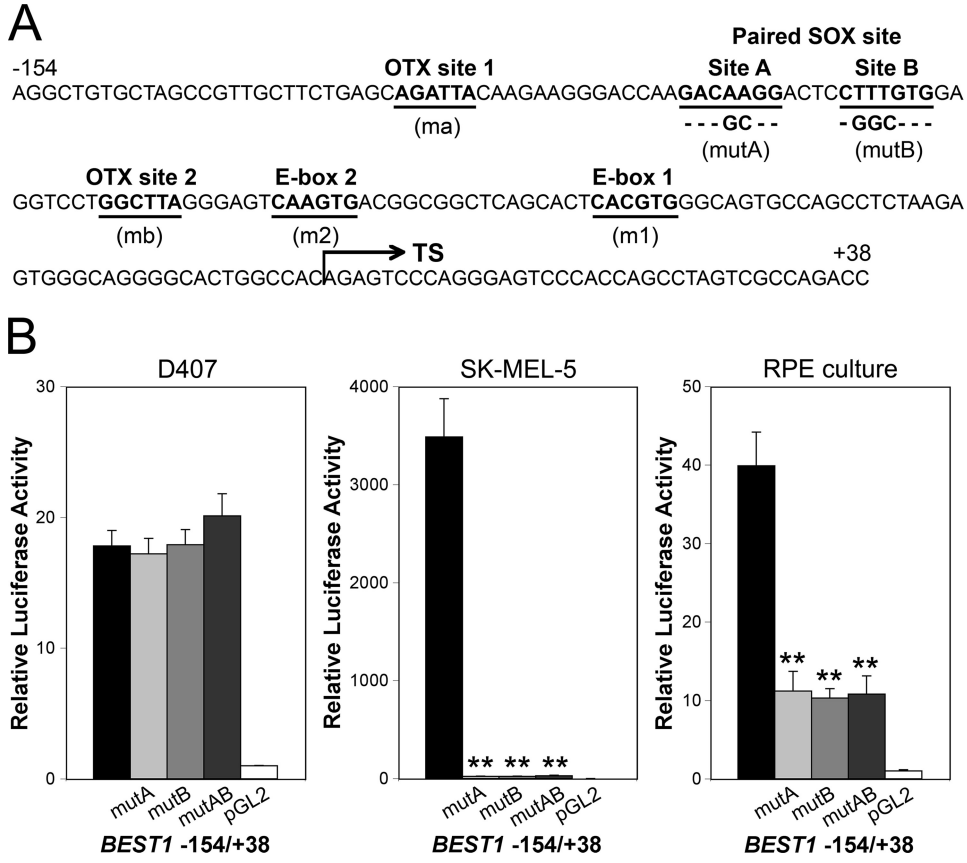

FIGURE 1. **Paired SOX site contributes to *BEST1* promoter activity.** *A*, nucleotide sequence of the *BEST1* −154 to +38 bp region. The transcription start site (*TS*; numbered +1) is indicated by an *angled arrow*. A paired SOX site (Sites A and B), two E-box sites (E-boxes 1 and 2), and two OTX sites (Sites 1 and 2) are highlighted in *boldface* and *underlined*. Mutation in the paired SOX site, Sites A and B, is indicated *under* the *boldfaced* sequence and designated mutA and mutB, respectively. Designation of mutation of E-boxes (m1 and m2) and OTX sites (ma and mb) is also indicated *under* each site. *B*, effect of mutation of the paired SOX site on *BEST1* promoter activity. Luciferase constructs containing wild-type sequence or mutation of the paired SOX site, Site A (mutA), Site B (mutB), or both (mutAB), in the context of the *BEST1* −154 to +38 bp promoter or an empty pGL2-Basic vector were transfected into host cells together with control pRL-CMV containing *Renilla* luciferase gene for normalization. As host cells, D407 human RPE cell line (*left panel*), SK-MEL-5 human melanoma cell line (*middle panel*), and pig RPE primary culture (*right panel*) were used. Dual luciferase assays were performed 48–60 h after transfection. Firefly luciferase activity was normalized by *Renilla* luciferase activity, and relative luciferase activity was calculated as the ratio of the normalized luciferase activity with constructs containing *BEST1* promoter fragments to that with empty pGL2-Basic. Transfection experiments were performed four times with D407 and SK-MEL-5 and five times with pig RPE primary cells in duplicate each time. The values represent the means and S.E. (*bar*). Statistical significance was examined for each mutated construct compared with the wild-type construct and is shown by ** ($p < 0.01$).

expressed at some levels in the RPE as well. Based on these expression patterns, SOX9 seemed to be the most relevant factor in the RPE, although the involvement of SOX10 still needed to be considered.

SOX9, but Not SOX10, Binds to BEST1 Proximal Promoter in Vivo in RPE—To determine more definitively which transcription factor, SOX9 or SOX10, is biologically relevant to the regulation of *BEST1* in the RPE, we performed ChIP with fresh bovine RPE cells to test binding of SOX9 and SOX10 to the *BEST1* promoter *in vivo*. Three independent ChIP experiments with the anti-SOX9 antibody AB5535 consistently yielded the highest peak of relative enrichment at *BEST1* −100 bp with no enrichment at the upstream and downstream regions in the RPE (Fig. 2*A*). In contrast, ChIP with either the anti-SOX10 antibody sc-17342 or ab25978 showed no peak of enrichment throughout the *BEST1* genomic locus (Fig. 2*A*), although both antibodies were successfully used in ChIP with rat sciatic nerves and the S16 rat Schwann cell line (63, 64). As control, ChIP with bovine retina in which *BEST1* is not expressed showed no peak of enrichment in the *BEST1* genomic region using the same anti-SOX9 antibody, AB5535 (Fig. 2*B*). The SOX9 binding location was further analyzed with higher resolution using primers located between *BEST1* −400 and +200 bp. A peak of relative enrichment was obtained at −100 bp where the paired SOX site is in fact localized with significantly lower enrichment observed at ~150 and 250 bp upstream ($p = 0.028$ and $p = 0.0097$, respectively) and downstream ($p = 0.020$ and $p = 0.0085$, respectively) from the peak (Fig. 2*C*). As for the antibodies used, the specificity of the AB5535 antibody was previously demonstrated by immunohistochemistry of retinal sections in which SOX9 staining in Müller glia was abrogated in conditional *Sox9* knock-out mice (19). The sc-17342 and ab25978 antibodies were both polyclonal and generated using human SOX10 peptides of 20 (N-terminal) and 50 (at 178–227 amino acid position) amino acids, respectively (63, 64). Because the sequences of these peptides are identical and have a mismatch by one amino acid between human and bovine, respectively, these antibodies are expected to react with bovine SOX10 as well. These results indicate that SOX9, but not SOX10, binds to the location around the paired SOX site in the *BEST1* promoter in RPE cells.

SOX9 Transactivates BEST1 Promoter through Paired SOX Site—Based on the ChIP results combined with the high and selective expression in the RPE, SOX9 seemed to be the most biologically relevant factor to *BEST1* regulation, and therefore, we focused on SOX9 in subsequent studies. Because the *BEST1* paired SOX site was functional in cells expressing the SOX-E factors with Sites A and B being equally important, we first tested whether exogenously introduced SOX9 also functions in the same manner. Cotransfection assays were performed in D407 cells using a human SOX9 expression vector and the *BEST1*−154/+38-luciferase constructs with wild-type sequence or mutation of the paired SOX site. SOX9 activated the wild-type *BEST1* promoter, and all mutations, mutA, mutB, and mutAB, significantly decreased the transactivation down to 26% ($p = 0.00012$), 21% ($p = 0.00004$), and 19% ($p = 0.00003$) of that of the wild-type construct, respectively (Fig. 3*A*), indicating

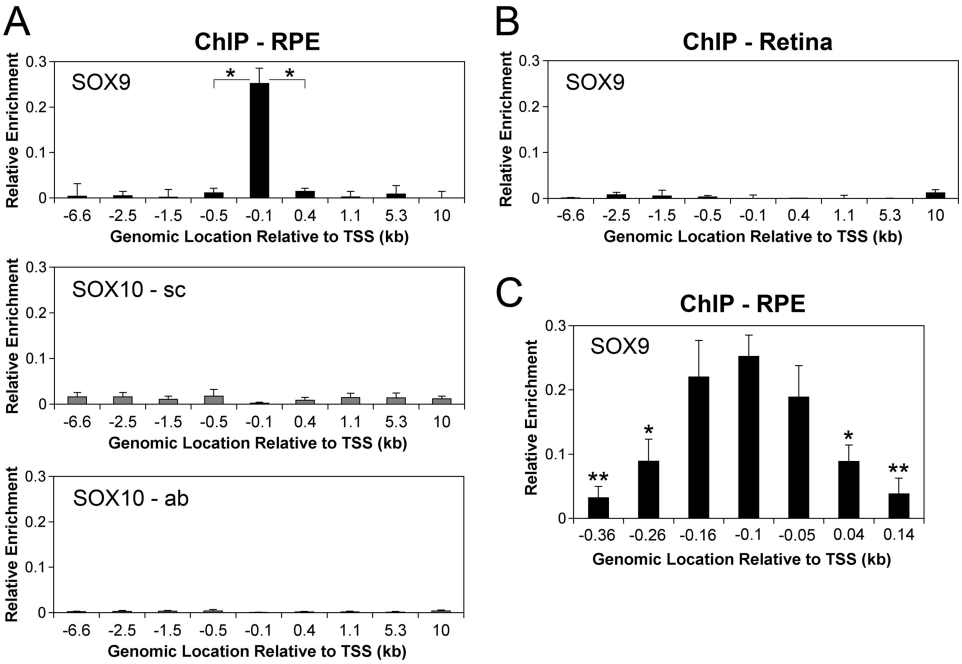

FIGURE 2. **SOX9 binds to *BEST1* proximal promoter *in vivo* in RPE.** *A*, ChIP for SOX9 and SOX10 with bovine RPE. ChIP was performed using fresh bovine RPE cells with anti-SOX9 antibody AB5535 or anti-SOX10 antibody sc-17342 (labeled *sc*) or ab25978 (labeled *ab*). The final DNA precipitates and diluted input (1:50) were analyzed by qPCR in duplicate with primers amplifying 100–200-bp fragments in different regions of *BEST1* as indicated upstream (labeled −) and downstream (labeled +) from the transcription start site (*TSS*). Relative enrichment at each genomic region was calculated as the ratio of the amount of PCR template in ChIP samples to that in diluted input. ChIP experiments were performed three times independently, and the means and S.E. (*bar*) were calculated from three ChIP results for each genomic location. Statistical significance was analyzed for a location next to the peak at each side and is shown by * ($p < 0.05$). *B*, ChIP for SOX9 with bovine retina. ChIP was performed, and results are presented in the same manner as described in *A* except that only the anti-SOX9 antibody AB5535 was used with fresh bovine retina. *C*, ChIP analysis of SOX9 binding with higher resolution. The ChIP samples obtained in *A* with the anti-SOX9 antibody were further analyzed by qPCR to narrow down the SOX9 binding location. Results are presented in the same manner as described in *A*. A peak of relative enrichment was still obtained at *BEST1* −100 bp with significantly lower enrichment observed at upstream and downstream regions from the peak. Statistical significance was analyzed for each location compared with the peak at −100 bp and is presented by * ($p < 0.05$) and ** ($p < 0.01$).

that Sites A and B are equally important. In addition, the pattern and degree of reduction by the mutated constructs were strikingly similar to the effects of these constructs introduced into pig RPE primary cultures (Fig. 1*B*).

SOX9 Knockdown Decreases BEST1 Promoter Activity—To complement the gain-of-function study that potentially involved an amount of SOX9 protein above physiological levels, we took a loss-of-function approach using siRNA to test the effects of reducing the SOX9 level on *BEST1* promoter activity in pig RPE primary cells. First, we checked the transfection efficiency using fluorescein-labeled RNA oligonucleotides, and it was ~50% (data not shown). Next, we checked the knockdown efficiency by RT-qPCR of custom-made siRNAs 1, 2, and 3 for pig *SOX9* at different concentrations and chose 100 nM for all experiments. Although *SOX9* mRNA levels were decreased only by siRNA 1, but not by siRNA 2 or 3, we decided to use all siRNAs with siRNAs 2 and 3 serving as negative controls. Treatment with siRNA 1 decreased *SOX9* mRNA levels down to 45% ($p = 0.000008$) of that without siRNA (Fig. 3*B*, *left panel*), and promoter activity in *BEST1*−154/+38-luciferase was reduced to 64% ($p = 0.017$) of control (Fig. 3*B*, *right panel*). In contrast, siRNAs 2 and 3 showed no reduction in either assay. *SOX10* mRNA levels were not affected in these conditions (data not shown).

SOX9 Physically Interacts with MITF and OTX2—Because SOX9 was reported to interact with other transcription factors (65), we hypothesized that SOX9 might also interact with MITF and OTX2, which we previously defined as regulators of *BEST1* (16, 17). To test this hypothesis, we first examined physical interactions by *in vitro* co-immunoprecipitation using proteins generated by *in vitro* transcription and translation. A combination of proteins (indicated by + in Fig. 4), non-labeled (no mark) and [^{35}S]methionine-labeled (marked by *), were mixed and precipitated with the antibody indicated. To check the quality and quantity of input proteins, 1 μl of each labeled protein was also analyzed. We obtained clear bands, indicating that SOX9 interacted with MITF and OTX2 and vice versa but not with luciferase protein (Fig. 4). Combined with the ChIP results for SOX9 described above and those for MITF and OTX2 reported (16, 17), the co-immunoprecipitation results raise the possibility that SOX9, MITF, and OTX2 may form a protein complex at the *BEST1* promoter in the RPE.

SOX9 Cooperatively Activates BEST1 Promoter with MITF and OTX2—Next, we examined functional interactions of SOX9 with MITF and OTX2 by cotransfection assays. *BEST1*−154/+38-luciferase constructs with wild-type sequence or mutation of the paired SOX site (mutA, mutB, or mutAB), E-boxes (m1, m2, or m1m2), or OTX sites (ma, mb, or mamb) (Fig. 1*A*) (16, 17) were transfected into D407 cells with various combinations of expression vectors for SOX9, MITF, and OTX2. With the wild-type *BEST1* promoter, although it was modestly activated by each single factor, synergistic activation was observed by a combination of SOX9 with MITF or OTX2 ($p = 0.00028$ with MITF; $p = 0.0041$ with OTX2) (Fig. 5). Synergistic activation was not observed between MITF and OTX2, and a combination of the three factors did not further stimulate the *BEST1* promoter beyond the level achieved by SOX9 with MITF. The synergistic effects by SOX9 with MITF or OTX2 required both Sites A and B of the paired SOX site (Fig. 5*A*). The effects of mutation of E-boxes and OTX sites were more complicated. In the presence of both SOX9 and OTX2, m1 increased *BEST1* promoter activity, but m2 and m1m2 had lesser or no effects (Fig. 5*B*). Of interest, non-canonical E-box 2 was more important than canonical E-box 1 for cooperation between SOX9 and MITF (Fig. 5*B*). Similarly, non-canonical OTX Site 2 was more important than canonical Site 1 for cooperation between SOX9 and OTX2 as well as by the three factors (Fig. 5*C*). Of further

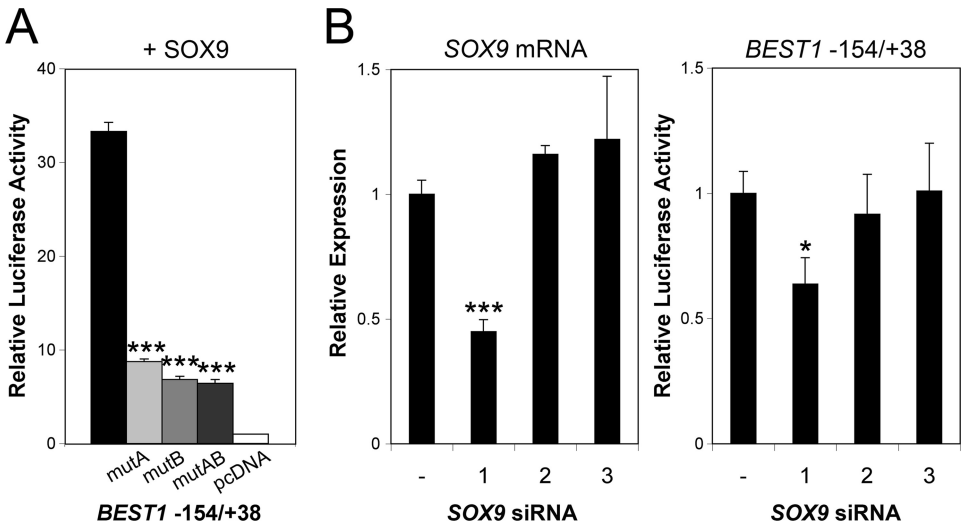

FIGURE 3. **Analyses using overexpression and knockdown approaches indicate SOX9 as regulator of *BEST1*.** *A*, SOX9 transactivates the *BEST1* promoter through the paired SOX site. *BEST1*−154/+38-luciferase constructs containing wild-type sequence or mutation of the paired SOX site (mutA, mutB, or mutAB) were transfected into D407 cells together with a human SOX9 expression vector or empty pcDNA3.1 as well as control pRL-TK containing *Renilla* luciferase gene for normalization. Firefly luciferase activity was normalized by *Renilla* luciferase activity, and relative luciferase activity was calculated as the ratio of the normalized luciferase activity with SOX9 to that with empty pcDNA3.1 (defined as 1) for each luciferase construct. Transfection experiments were performed five times in quadruplicate each time. The values represent the means and S.E. (*bar*). Statistical significance was examined for each mutated construct compared with the wild-type construct and is shown by *** ($p < 0.001$). *B*, SOX9 knockdown decreases *BEST1* promoter activity. *Left panel*, custom-made siRNAs 1, 2, and 3 for pig *SOX9* (supplemental table) were transfected into pig RPE primary cells at a final concentration of 100 nM, and total RNAs were extracted 36 h after transfection. The efficiency of *SOX9* knockdown was evaluated by RT-qPCR with primers specific for pig *SOX9* and *GAPDH*. The mRNA level of *SOX9* was normalized by that of *GAPDH*, and relative expression was calculated as the ratio of the normalized expression level with siRNA to that without siRNA (labeled −; presented as 1). The values represent the means and S.E. (*bar*) of five experiments. Statistical significance was analyzed for relative expression with each siRNA compared with that without siRNA and is presented by *** ($p < 0.001$). *Right panel*, double transfections were performed sequentially, first with *SOX9* siRNAs and then 24 h later with plasmid DNA containing the *BEST1*−154/+38-luciferase construct and control pRL-TK. Dual luciferase assays were performed 48–60 h after plasmid transfection. Firefly luciferase activity was normalized by *Renilla* luciferase activity, and relative luciferase activity was calculated as the ratio of the normalized luciferase activity with siRNA to that without siRNA (presented as 1). The values represent the means and S.E. (*bar*) of eight experiments. Statistical significance was examined for relative luciferase activity with each siRNA compared with that without siRNA and is presented by * ($p < 0.05$).

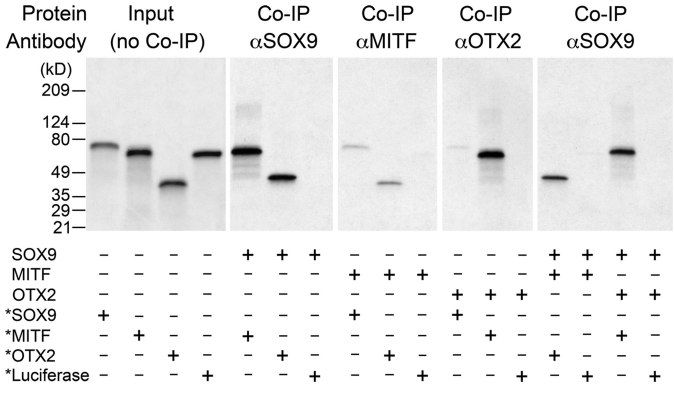

FIGURE 4. **SOX9 physically interacts with MITF and OTX2.** *In vitro* co-immunoprecipitation (*Co-IP*) was performed using proteins generated by *in vitro* transcription and translation for human SOX9, MITF, OTX2, and control luciferase. Proteins, 15 μl each of non-labeled (no mark) and [^{35}S]methionine-labeled (marked by *), were mixed (indicated by +) to form a protein complex; incubated with anti-SOX9, anti-MITF, or anti-OTX2 antibody; and precipitated by Protein A-Sepharose. Bound proteins were eluted and resolved by SDS-PAGE followed by autoradiography. To check the quality of input proteins, 1 μl of labeled proteins was also analyzed in parallel. Bands indicate interaction of proteins in the mixture.

interest, although mutation of the paired SOX site and to a lesser degree mutation of the OTX sties significantly reduced transactivation by the three factors, mutation of the E-boxes did not decrease *BEST1* promoter activity in this condition. These results suggest that the paired SOX site has a more central role in the cooperation of SOX9, MITF, and OTX2 than the E-boxes or OTX sites and that the E-boxes are not required for cooperation of the three factors.

Combination of Expression Patterns of SOX9, MITF, and OTX2 Predicts RPE-predominant Expression of BEST1—SOX9, MITF, and OTX2 interact with each other and regulate *BEST1*. To make this scenario happen, obviously their expression should be overlapped in the RPE. We therefore analyzed additionally the expression of *MITF*, *OTX2*, and *BEST1* by RT-qPCR using the same set of RNA samples as used for the SOX-E genes (supplemental Fig. S2). *MITF*, including all isoforms, was expressed in many tissues at various levels with high expression in SK-MEL-5, small intestine, heart, and RPE (Fig. 6). *OTX2* expression was mostly confined to RPE, retina, and RPE primary cells. *BEST1* expression was most impressive in that it was highly and selectively expressed in the RPE with barely detectable expression in the testis and brain (Fig. 6). None of the expression patterns of a single transcription factor mimicked that of *BEST1*. Therefore, we hypothesized that multiple factors form a putative regulatory complex that is unique to the RPE and function together to achieve the exquisite tissue specificity of *BEST1* expression. To test this hypothesis, we combined the expression patterns of two or three factors by multiplying their expression levels. Although all two-factor combinations yielded the expression patterns preferentially in the RPE, they still showed some expression in other tissues. In contrast, a combination of the three factors resulted in the RPE-predominant expression pattern that was remarkably similar to that of *BEST1*, suggesting that combinatorial regulation is likely at work on *BEST1* expression.

BEST1 Promoter Is Active in Sertoli Cells of Testis—Because SOX9 seemed to play a key role in regulating *BEST1* in the RPE, we hypothesized that SOX9 may also regulate *BEST1* in other cell types in which SOX9 is expressed. Based on the well known expression and functional importance of SOX9 in Sertoli cells of the testis, we analyzed lacZ expression in the testis of transgenic mice that carried a *lacZ* reporter driven by the *BEST1* −424 to +38 bp promoter (18). We first confirmed the characteristic distribution of Sertoli cells by SOX9 immunohistochemistry (Fig. 7*A*). Then, lacZ expression was analyzed by staining with X-Gal, and blue staining was observed in a distri-

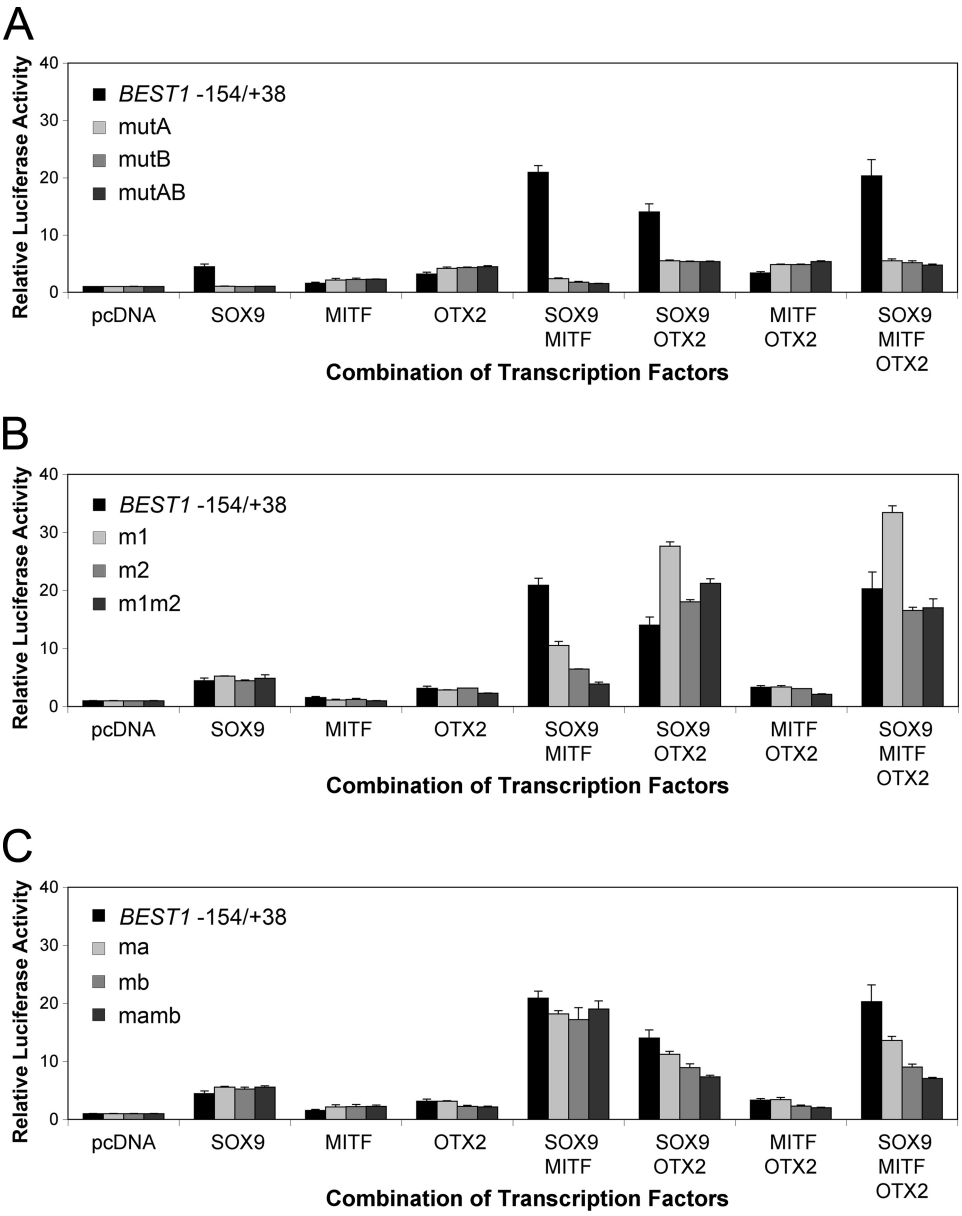

FIGURE 5. **SOX9 cooperatively activates *BEST1* promoter with MITF and OTX2.** *A*, effects of mutation of the paired SOX site on *BEST1* promoter activity. Cotransfection assays were performed in D407 cells using *BEST1*−154/+38-luciferase constructs with wild-type sequence or mutation of the paired SOX site (mutA, mutB, or mutAB) and various combinations of expression vectors for human SOX9, MITF, and OTX2 together with control pRL-TK for normalization. The total amount of expression vectors was adjusted to 1.5 μg for all combinations by adding empty pcDNA3.1 plasmid. Firefly luciferase activity was normalized by *Renilla* luciferase activity, and relative luciferase activity was calculated as the ratio of the normalized luciferase activity with the expression vectors to that with empty pcDNA3.1 (defined as 1) for each luciferase construct. Transfection experiments were performed three times independently in duplicate each time, and the values represent the means and S.E. (*bar*). *B*, effects of mutation of the E-boxes on *BEST1* promoter activity. Experiments were performed and results are presented in the same manner as described in *A* except that *BEST1*−154/+38-luciferase constructs with mutation of the E-boxes (m1, m2, or m1m2) were used. *C*, effects of mutation of the OTX sites on *BEST1* promoter activity. Experiments were performed and results are presented in the same manner as described in *A* except that *BEST1*−154/+38-luciferase constructs with mutation of the OTX sites (ma, mb, or mamb) were used.

bution pattern similar to that of SOX9 (Fig. 7*B*). These results indicate that the *BEST1* promoter is active in Sertoli cells and suggest for the first time *BEST1* expression in this cell type where SOX9 is highly expressed.

DISCUSSION

Our previous studies showed that the *BEST1* −154 to +38 bp region is sufficient to direct expression in the RPE, and MITF and OTX2 regulate this promoter (16, 17). However, a number of questions still remained. Here, we have described the identification of SOX9 as a transcription factor that binds to this *BEST1* promoter and functions cooperatively with MITF and OTX2 in the RPE. Although the expression of SOX9 in the RPE has recently been discovered (19), its function in this cell type has never been described. Therefore, this is the first report showing the functional role of SOX9 in the RPE. The identification of SOX9 as a key regulator of *BEST1* not only provides a new clue as to how *BEST1* is regulated in the RPE and thereby answers some of the questions raised in our previous studies as discussed below but also finds an important missing piece in the RPE regulatory network in general, opening doors to deeper understanding of RPE biology.

It was initially reported that the regulatory region of some SOX9 target genes, such as mouse *Col11a2*, contains paired SOX sites to which SOX9 binds as a dimer and that this DNA-dependent dimerization is critical for chondrogenesis but not for sex determination (40, 41, 45). Subsequently, however, a so-called paired SOX site has also been found in the regulatory region of the genes important for testis development, such as mouse *Amh* and *Ptgds*, with two binding elements in opposite orientation separated by 3–4 bp spacing (41, 42, 44, 46). The paired SOX site in the *BEST1* promoter has the same characteristic arrangement. Therefore, the paired arrangement of SOX sites may be more common than originally reported.

The existence of the paired SOX site prompted us to reexamine the spatial relationship of binding sites for SOX9, MITF, and OTX2 in the *BEST1*−154 to +38 bp region. In our previous studies, it was puzzling that the non-canonical sites, E-box 2 for MITF and OTX Site 2 for OTX2, were equally and more functionally important than the canonical E-box 1 and OTX Site 1, respectively, despite weaker binding of the non-canonical sites in *in vitro* binding assays (16, 17). It turned out that E-box 2 and OTX Site 2 are located in greater proximity to the paired SOX site than E-box 1 and OTX Site 1,

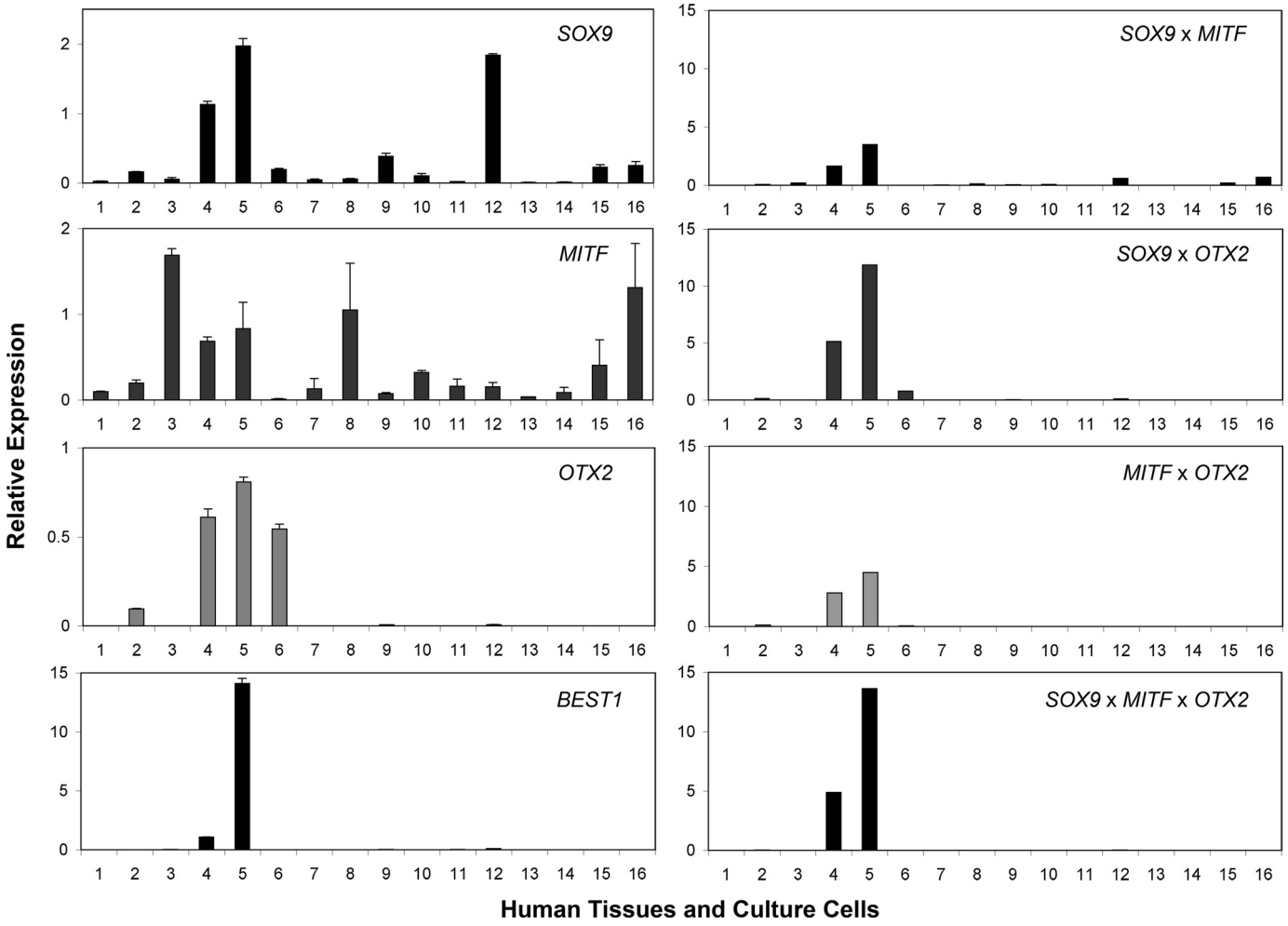

FIGURE 6. **Combination of expression patterns of *SOX9*, *MITF*, and *OTX2* predicts *BEST1* expression in RPE.** *Left panel*, the expression levels of *SOX9*, *MITF*, *OTX2*, *BEST1*, and control *GAPDH* were analyzed by RT-qPCR using RNAs from 10 human tissues (purchased) and RNAs extracted from human RPE, retina, and four cell cultures. The expression level of each gene was normalized by that of *GAPDH* and presented as relative expression. The values represent the means and S.E. (*bar*) of qPCR results in triplicate. *Right panel*, to combine the expression patterns of multiple genes, relative expression in each sample (E_S: sample) was summed for all samples (E_T: total) for each gene. Then, E_S/E_T was calculated for each gene and multiplied by 10, and the resultant values for *SOX9*, *MITF*, and/or *OTX2* were multiplied for each sample. Samples are as follows: D407 (*1*), ARPE19 (*2*), SK-MEL-5 (*3*), M1 (*4*), RPE (*5*), retina (*6*), liver (*7*), heart (*8*), brain (*9*), kidney (*10*), spleen (*11*), testis (*12*), thymus (*13*), bone marrow (*14*), colon (*15*), and small intestine (*16*).

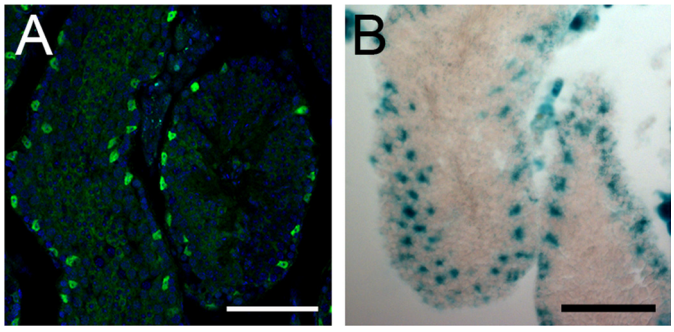

FIGURE 7. ***BEST1* promoter is active in Sertoli cells of testis in transgenic mice.** *A*, SOX9 expression in the testis by immunohistochemistry. The testis of transgenic mice carrying a *lacZ* reporter driven by the *BEST1* −424 to +38 bp promoter was histologically analyzed for SOX9 expression. Sections were cut at 10 μm, fixed in 1% paraformaldehyde in PBS, blocked in 10% horse serum, and incubated with anti-SOX9 antibody AB5535 in 3% horse serum at 4 °C overnight, and the SOX9 antibody was detected with anti-rabbit IgG antibody conjugated with Alexa Fluor 488 (*green* fluorescence). The sections were mounted in DAPI-containing mounting medium (*blue* fluorescence). *White horizontal bar*, 100 μm. *B*, lacZ expression in the testis by X-Gal staining. Sections prepared from the same transgenic mouse testis were fixed in 0.5% glutaraldehyde in PBS and stained with X-Gal at 37 °C for 18 h. *Black horizontal bar*, 100 μm.

respectively. Importantly, all binding sites for the three factors in the *BEST1* promoter are completely conserved between human and bovine. Considering that SOX9 physically interacts with MITF and OTX2, we speculate that the spatial proximity may make E-box 2 and OTX Site 2 functionally more important through cooperative binding, resulting in synergistic activation. Interestingly and potentially supporting this speculation, transactivation of the *BEST1* promoter with the three factors was not decreased by mutation of E-box 1 when E-box 2 was intact. Likewise, transactivation of the *BEST1* promoter with the three factors was more clearly decreased by mutation of OTX Site 2 but only slightly decreased by mutation of OTX Site 1. Because MITF bound only marginally to E-box2 in *in vitro* binding assays, we previously assumed that E-box 2 should be bound by different factors other than MITF (16). However, YOH screen with bait containing E-box 2 also isolated multiple clones encoding MITF and TFE3 but not other transcription factors,[3] supporting E-box 2 as a binding site for MITF. An intriguing

[3] N. Esumi, unpublished results.

observation is that mutation of E-box 1 rather increased *BEST1* promoter activity with SOX9 and OTX2 or the three factors. This mutation would prevent factors such as MITF from binding to the canonical E-box 1 and thereby increase their availability for binding to E-box 2, or MITF might function as a cofactor for the SOX9-OTX2 complex without binding to DNA as it is reported that MITF can function as a non-DNA binding cofactor for LEF1 through physical interaction (66).

Another question for which the present study might give a better explanation is why *BEST1* promoter activity is substantially higher (200–300-fold) in SK-MEL-5 than in D407. We previously attributed this difference to the considerably higher level of endogenous MITF in SK-MEL-5 (16). However, based on the present study, such high *BEST1* promoter activity in SK-MEL-5 seems more attributable to a combination of the high levels of MITF and SOX10, another SOX-E factor that shares the binding sequence. It is reported that *Dct* expression is synergistically activated by SOX10 and MITF in mouse melanocyte development (67). In matured human skin melanocytes, ultraviolet B radiation increases the expression of SOX9, which directly regulates *MITF*, and then SOX9 and MITF act together to activate the *DCT* promoter, leading to melanin production (38). In these *Dct*/*DCT* promoters, binding sites for MITF and SOX10/SOX9 are ~300 bp apart, and it is unclear whether these factors directly interact with each other. Nevertheless, the present study disclosed another regulatory component that is shared by melanocytes and RPE cells because the SOX-E factors have been extensively studied in melanocytes but not in the RPE to date. Yet these two cell types are very different in many aspects, such as origin, morphology, gene expression, and function, with OTX2 expressed only in the RPE as one example. Our results show that combinatorial regulation by the shared (SOX9 and MITF) and unique (OTX2) factors can achieve the exquisite tissue specificity of *BEST1* expression in the RPE.

Although the present study defined SOX9 as a key regulator of *BEST1*, we cannot exclude the possibility that SOX8 may still play some role in the regulation of *BEST1* even at the lower level of expression in the RPE. Functional compensation and redundancy were observed among the SOX-E factors in other cell types, such as redundant functions between SOX8 and SOX9 in Sertoli cells of the testis and between SOX8 and SOX10 in oligodendrocytes of the spinal cord (68–71). However, the functional redundancy is not complete, and each factor has its own distinct functions (69, 71). In addition, even if multiple SOX-E factors are expressed in the same cell type, all factors are not equally important. For example, SOX8 and SOX9 are expressed in the testis, but SOX9 plays more critical roles in early testis development as heterozygous mutation of human *SOX9* causes XY sex reversal (23, 34, 35). In contrast, in mice, even homozygous deletion of *Sox8* results in no embryonic or early postnatal phenotype other than an idiopathic weight reduction (72). Furthermore, SOX10 is also expressed in the testis, but no function has been found so far (23). In light of these examples, our detection of *SOX10* expression in the RPE may not be simply due to contamination of choroidal melanocytes in RPE samples; rather, *SOX10* may be indeed expressed in the RPE with no significant role, if any, in the regulation of *BEST1*. At this point, therefore, biological roles of additional SOX-E factors in the RPE are unclear.

It is intriguing that SOX9 activates the expression of *Ptgds*, the gene encoding prostaglandin D_2 synthase that isomerizes prostaglandin H_2 to prostaglandin D_2 (PGD_2), and thereby leads to the accumulation of PGD_2 in Sertoli cells. Then, PGD_2 in turn activates transcription and nuclear translocation of SOX9, forming a feed forward loop in testis development (46, 73). The PGD_2-mediated SOX9 nuclear localization is an important timing checkpoint for testis development because SOX9 initially accumulates in the cytoplasm until the critical time to begin its regulatory function in the nucleus (74). Here, two questions arise. Is *PTGDS* regulated by SOX9 in the RPE as well? Our preliminary results suggest that it is the case.[3] If so, is a similar regulatory loop between SOX9 and PGD_2 operating in the RPE? Both are important questions because *PTGDS* is among the genes that are expressed at the highest levels in the RPE, the first and fourth in mouse and human, respectively (NEIBank, National Institutes of Health) (75, 76). However, neither its functional role nor regulation has been described in the RPE. It seems worthwhile to explore the connection between SOX9 and PGD_2 as well as the function of the PGD_2 pathway in the RPE.

Besides *PTGDS*, we hypothesized that additional SOX9 target genes may be shared by the RPE and other cell types expressing SOX9, and *BEST1* seemed to be a good candidate for such a gene. We explored this possibility and found that the *BEST1* promoter was active in Sertoli cells in transgenic mice, suggesting for the first time *BEST1* expression in Sertoli cells. In addition, there are at least two reports for *BEST1* as such an example. A transgenic mouse line expressing Cre recombinase in retinal Müller glia was found when making inducible RPE-specific Cre mice using the *BEST1* promoter (77). Bestrophin-1 was found as a Ca^{2+}-activated anion channel in hippocampal astrocytes where SOX9 is also expressed (49). The list of specific cell types in which both *BEST1* and SOX9 are expressed will be growing.

Most CD patients die during the neonatal period due to respiratory distress with 5–10% surviving infancy (34, 35). Because of such severe symptoms, little attention has been paid to other phenotypes such as eye problems. In surviving CD patients, eye problems reported are mostly myopia; however, the phenotype of surviving CD patients would not represent the entire spectrum of SOX9 functions in the eye. Homozygous *Sox9* knock-out mice cannot be produced because healthy and fertile heterozygous *Sox9* knock-outs cannot be obtained (36). At this time, therefore, the real impact of SOX9 deletion on eye development and function is unclear. There is a mouse model for SOX9 overexpression in the RPE that was generated coincidentally when making transgenic mice carrying a tyrosinase minigene driven by the *Dct* promoter (78, 79). In these *Odd Sex* (*Ods*) mice, which show pigmentation defects and XX sex reversal, the transgene is inserted 0.98 Mb upstream of *Sox9*. Of great interest, this insertion also causes microphthalmia due to the inappropriate expression of *Sox9* in the RPE driven by the *Dct* promoter through long range activation (79). For loss-of-function analysis, *Sox9* conditional knock-outs targeting RPE cells are necessary, and such studies should be carried out in the

future. Furthermore, to understand the roles of SOX9 in matured RPE cells, a strategy that allows analysis of the effects of SOX9 deletion in adult animals without affecting development, such as an inducible conditional knock-out approach (80), will be desirable. Future studies will bring us exciting findings and new insights into RPE development and function.

Acknowledgment—We thank Dr. Valerie Fontaine (Fovea Pharmaceuticals, Paris, France) for a protocol for pig RPE primary culture.

REFERENCES

1. Bok, D. (1993) *J. Cell Sci. Suppl.* **17,** 189–195
2. Thumann, G., and Hinton, D. R. (2001) in *Retina* (Ryan, S. J., ed) 3rd Ed., Vol. 3, pp. 104–121, Mosby, St. Louis, MO
3. Goding, C. R. (2000) *Genes Dev.* **14,** 1712–1728
4. Steingrímsson, E., Copeland, N. G., and Jenkins, N. A. (2004) *Annu. Rev. Genet.* **38,** 365–411
5. Bharti, K., Nguyen, M. T., Skuntz, S., Bertuzzi, S., and Arnheiter, H. (2006) *Pigment Cell Res.* **19,** 380–394
6. Hemesath, T. J., Steingrímsson, E., McGill, G., Hansen, M. J., Vaught, J., Hodgkinson, C. A., Arnheiter, H., Copeland, N. G., Jenkins, N. A., and Fisher, D. E. (1994) *Genes Dev.* **8,** 2770–2780
7. Hodgkinson, C. A., Moore, K. J., Nakayama, A., Steingrímsson, E., Copeland, N. G., Jenkins, N. A., and Arnheiter, H. (1993) *Cell* **74,** 395–404
8. Nakayama, A., Nguyen, M. T., Chen, C. C., Opdecamp, K., Hodgkinson, C. A., and Arnheiter, H. (1998) *Mech. Dev.* **70,** 155–166
9. Nguyen, M., and Arnheiter, H. (2000) *Development* **127,** 3581–3591
10. Bovolenta, P., Mallamaci, A., Briata, P., Corte, G., and Boncinelli, E. (1997) *J. Neurosci.* **17,** 4243–4252
11. Martínez-Morales, J. R., Rodrigo, I., and Bovolenta, P. (2004) *BioEssays* **26,** 766–777
12. Martinez-Morales, J. R., Signore, M., Acampora, D., Simeone, A., and Bovolenta, P. (2001) *Development* **128,** 2019–2030
13. Matsuo, I., Kuratani, S., Kimura, C., Takeda, N., and Aizawa, S. (1995) *Genes Dev.* **9,** 2646–2658
14. Simeone, A., Puelles, E., and Acampora, D. (2002) *Curr. Opin. Genet. Dev.* **12,** 409–415
15. Martínez-Morales, J. R., Dolez, V., Rodrigo, I., Zaccarini, R., Leconte, L., Bovolenta, P., and Saule, S. (2003) *J. Biol. Chem.* **278,** 21721–21731
16. Esumi, N., Kachi, S., Campochiaro, P. A., and Zack, D. J. (2007) *J. Biol. Chem.* **282,** 1838–1850
17. Esumi, N., Kachi, S., Hackler, L., Jr., Masuda, T., Yang, Z., Campochiaro, P. A., and Zack, D. J. (2009) *Hum. Mol. Genet.* **18,** 128–141
18. Esumi, N., Oshima, Y., Li, Y., Campochiaro, P. A., and Zack, D. J. (2004) *J. Biol. Chem.* **279,** 19064–19073
19. Poché, R. A., Furuta, Y., Chaboissier, M. C., Schedl, A., and Behringer, R. R. (2008) *J. Comp. Neurol.* **510,** 237–250
20. Bowles, J., Schepers, G., and Koopman, P. (2000) *Dev. Biol.* **227,** 239–255
21. Harley, V. R., Clarkson, M. J., and Argentaro, A. (2003) *Endocr. Rev.* **24,** 466–487
22. Schepers, G. E., Teasdale, R. D., and Koopman, P. (2002) *Dev. Cell* **3,** 167–170
23. Barrionuevo, F., and Scherer, G. (2010) *Int. J. Biochem. Cell Biol.* **42,** 433–436
24. Koopman, P. (2005) *Trends Genet.* **21,** 367–370
25. Sekido, R., and Lovell-Badge, R. (2008) *Nature* **453,** 930–934
26. Wilhelm, D., Martinson, F., Bradford, S., Wilson, M. J., Combes, A. N., Beverdam, A., Bowles, J., Mizusaki, H., and Koopman, P. (2005) *Dev. Biol.* **287,** 111–124
27. Akiyama, H. (2008) *Mod. Rheumatol.* **18,** 213–219
28. Akiyama, H., Chaboissier, M. C., Martin, J. F., Schedl, A., and de Crombrugghe, B. (2002) *Genes Dev.* **16,** 2813–2828
29. Seymour, P. A., Freude, K. K., Dubois, C. L., Shih, H. P., Patel, N. A., and Sander, M. (2008) *Dev. Biol.* **323,** 19–30
30. Seymour, P. A., Freude, K. K., Tran, M. N., Mayes, E. E., Jensen, J., Kist, R., Scherer, G., and Sander, M. (2007) *Proc. Natl. Acad. Sci. U.S.A.* **104,** 1865–1870
31. Stolt, C. C., Lommes, P., Sock, E., Chaboissier, M. C., Schedl, A., and Wegner, M. (2003) *Genes Dev.* **17,** 1677–1689
32. Stolt, C. C., and Wegner, M. (2010) *Int. J. Biochem. Cell Biol.* **42,** 437–440
33. Wegner, M., and Stolt, C. C. (2005) *Trends Neurosci.* **28,** 583–588
34. Foster, J. W., Dominguez-Steglich, M. A., Guioli, S., Kwok, C., Weller, P. A., Stevanović, M., Weissenbach, J., Mansour, S., Young, I. D., Goodfellow, P. N., Brook, J. D., and Schafer, A. J. (1994) *Nature* **372,** 525–530
35. Wagner, T., Wirth, J., Meyer, J., Zabel, B., Held, M., Zimmer, J., Pasantes, J., Bricarelli, F. D., Keutel, J., Hustert, E., Wolf, U., Tommerup, N., Schempp, W., and Scherer, G. (1994) *Cell* **79,** 1111–1120
36. Bi, W., Huang, W., Whitworth, D. J., Deng, J. M., Zhang, Z., Behringer, R. R., and de Crombrugghe, B. (2001) *Proc. Natl. Acad. Sci. U.S.A.* **98,** 6698–6703
37. Muto, A., Iida, A., Satoh, S., and Watanabe, S. (2009) *Exp. Eye Res.* **89,** 549–558
38. Passeron, T., Valencia, J. C., Bertolotto, C., Hoashi, T., Le Pape, E., Takahashi, K., Ballotti, R., and Hearing, V. J. (2007) *Proc. Natl. Acad. Sci. U.S.A.* **104,** 13984–13989
39. Bell, D. M., Leung, K. K., Wheatley, S. C., Ng, L. J., Zhou, S., Ling, K. W., Sham, M. H., Koopman, P., Tam, P. P., and Cheah, K. S. (1997) *Nat. Genet.* **16,** 174–178
40. Bernard, P., Tang, P., Liu, S., Dewing, P., Harley, V. R., and Vilain, E. (2003) *Hum. Mol. Genet.* **12,** 1755–1765
41. Bridgewater, L. C., Lefebvre, V., and de Crombrugghe, B. (1998) *J. Biol. Chem.* **273,** 14998–15006
42. Bridgewater, L. C., Walker, M. D., Miller, G. C., Ellison, T. A., Holsinger, L. D., Potter, J. L., Jackson, T. L., Chen, R. K., Winkel, V. L., Zhang, Z., McKinney, S., and de Crombrugghe, B. (2003) *Nucleic Acids Res.* **31,** 1541–1553
43. Lefebvre, V., Huang, W., Harley, V. R., Goodfellow, P. N., and de Crombrugghe, B. (1997) *Mol. Cell. Biol.* **17,** 2336–2346
44. Schepers, G., Wilson, M., Wilhelm, D., and Koopman, P. (2003) *J. Biol. Chem.* **278,** 28101–28108
45. Sock, E., Pagon, R. A., Keymolen, K., Lissens, W., Wegner, M., and Scherer, G. (2003) *Hum. Mol. Genet.* **12,** 1439–1447
46. Wilhelm, D., Hiramatsu, R., Mizusaki, H., Widjaja, L., Combes, A. N., Kanai, Y., and Koopman, P. (2007) *J. Biol. Chem.* **282,** 10553–10560
47. Petrukhin, K., Koisti, M. J., Bakall, B., Li, W., Xie, G., Marknell, T., Sandgren, O., Forsman, K., Holmgren, G., Andreasson, S., Vujic, M., Bergen, A. A., McGarty-Dugan, V., Figueroa, D., Austin, C. P., Metzker, M. L., Caskey, C. T., and Wadelius, C. (1998) *Nat. Genet.* **19,** 241–247
48. Duta, V., Szkotak, A. J., Nahirney, D., and Duszyk, M. (2004) *FEBS Lett.* **577,** 551–554
49. Park, H., Oh, S. J., Han, K. S., Woo, D. H., Park, H., Mannaioni, G., Traynelis, S. F., and Lee, C. J. (2009) *J. Neurosci.* **29,** 13063–13073
50. Hartzell, H. C., Qu, Z., Yu, K., Xiao, Q., and Chien, L. T. (2008) *Physiol. Rev.* **88,** 639–672
51. Sun, H., Tsunenari, T., Yau, K. W., and Nathans, J. (2002) *Proc. Natl. Acad. Sci. U.S.A.* **99,** 4008–4013
52. Marmorstein, L. Y., Wu, J., McLaughlin, P., Yocom, J., Karl, M. O., Neussert, R., Wimmers, S., Stanton, J. B., Gregg, R. G., Strauss, O., Peachey, N. S., and Marmorstein, A. D. (2006) *J. Gen. Physiol.* **127,** 577–589
53. Rosenthal, R., Bakall, B., Kinnick, T., Peachey, N., Wimmers, S., Wadelius, C., Marmorstein, A., and Strauss, O. (2006) *FASEB J.* **20,** 178–180
54. Yu, K., Xiao, Q., Cui, G., Lee, A., and Hartzell, H. C. (2008) *J. Neurosci.* **28,** 5660–5670
55. Allikmets, R., Seddon, J. M., Bernstein, P. S., Hutchinson, A., Atkinson, A., Sharma, S., Gerrard, B., Li, W., Metzker, M. L., Wadelius, C., Caskey, C. T., Dean, M., and Petrukhin, K. (1999) *Hum. Genet.* **104,** 449–453
56. Yardley, J., Leroy, B. P., Hart-Holden, N., Lafaut, B. A., Loeys, B., Messiaen, L. M., Perveen, R., Reddy, M. A., Bhattacharya, S. S., Traboulsi, E., Baralle, D., De Laey, J. J., Puech, B., Kestelyn, P., Moore, A. T., Manson, F. D., and Black, G. C. (2004) *Invest. Ophthalmol. Vis. Sci.* **45,** 3683–3689
57. Burgess, R., Millar, I. D., Leroy, B. P., Urquhart, J. E., Fearon, I. M., De Baere, E., Brown, P. D., Robson, A. G., Wright, G. A., Kestelyn, P., Holder, G. E., Webster, A. R., Manson, F. D., and Black, G. C. (2008) *Am. J. Hum.*

Genet. **82,** 19–31
58. Davidson, A. E., Millar, I. D., Urquhart, J. E., Burgess-Mullan, R., Shweikh, Y., Parry, N., O'Sullivan, J., Maher, G. J., McKibbin, M., Downes, S. M., Lotery, A. J., Jacobson, S. G., Brown, P. D., Black, G. C., and Manson, F. D. (2009) *Am. J. Hum. Genet.* **85,** 581–592
59. Zhang, Y., Stanton, J. B., Wu, J., Yu, K., Hartzell, H. C., Peachey, N. S., Marmorstein, L. Y., and Marmorstein, A. D. (2010) *Hum. Mol. Genet.* **19,** 1108–1118
60. Kachi, S., Esumi, N., Zack, D. J., and Campochiaro, P. A. (2006) *Gene Ther.* **13,** 798–804
61. Chen, S., and Zack, D. J. (2000) *Methods Enzymol.* **316,** 590–610
62. Qian, J., Esumi, N., Chen, Y., Wang, Q., Chowers, I., and Zack, D. J. (2005) *Nucleic Acids Res.* **33,** 3479–3491
63. Jang, S. W., and Svaren, J. (2009) *J. Biol. Chem.* **284,** 20111–20120
64. LeBlanc, S. E., Ward, R. M., and Svaren, J. (2007) *Mol. Cell. Biol.* **27,** 3521–3529
65. Wissmüller, S., Kosian, T., Wolf, M., Finzsch, M., and Wegner, M. (2006) *Nucleic Acids Res.* **34,** 1735–1744
66. Saito, H., Yasumoto, K., Takeda, K., Takahashi, K., Fukuzaki, A., Orikasa, S., and Shibahara, S. (2002) *J. Biol. Chem.* **277,** 28787–28794
67. Jiao, Z., Mollaaghababa, R., Pavan, W. J., Antonellis, A., Green, E. D., and Hornyak, T. J. (2004) *Pigment Cell Res.* **17,** 352–362
68. Barrionuevo, F., Georg, I., Scherthan, H., Lécureuil, C., Guillou, F., Wegner, M., and Scherer, G. (2009) *Dev. Biol.* **327,** 301–312
69. Kellerer, S., Schreiner, S., Stolt, C. C., Scholz, S., Bösl, M. R., and Wegner, M. (2006) *Development* **133,** 2875–2886
70. O'Bryan, M. K., Takada, S., Kennedy, C. L., Scott, G., Harada, S., Ray, M. K., Dai, Q., Wilhelm, D., de Kretser, D. M., Eddy, E. M., Koopman, P., and Mishina, Y. (2008) *Dev. Biol.* **316,** 359–370
71. Stolt, C. C., Lommes, P., Friedrich, R. P., and Wegner, M. (2004) *Development* **131,** 2349–2358
72. Sock, E., Schmidt, K., Hermanns-Borgmeyer, I., Bösl, M. R., and Wegner, M. (2001) *Mol. Cell. Biol.* **21,** 6951–6959
73. Moniot, B., Declosmenil, F., Barrionuevo, F., Scherer, G., Aritake, K., Malki, S., Marzi, L., Cohen-Solal, A., Georg, I., Klattig, J., Englert, C., Kim, Y., Capel, B., Eguchi, N., Urade, Y., Boizet-Bonhoure, B., and Poulat, F. (2009) *Development* **136,** 1813–1821
74. Malki, S., Nef, S., Notarnicola, C., Thevenet, L., Gasca, S., Méjean, C., Berta, P., Poulat, F., and Boizet-Bonhoure, B. (2005) *EMBO J.* **24,** 1798–1809
75. Ida, H., Boylan, S. A., Weigel, A. L., Smit-McBride, Z., Chao, A., Gao, J., Buchoff, P., Wistow, G., and Hjelmeland, L. M. (2004) *Mol. Vis.* **10,** 439–444
76. Wistow, G., Bernstein, S. L., Wyatt, M. K., Fariss, R. N., Behal, A., Touchman, J. W., Bouffard, G., Smith, D., and Peterson, K. (2002) *Mol. Vis.* **8,** 205–220
77. Ueki, Y., Ash, J. D., Zhu, M., Zheng, L., and Le, Y. Z. (2009) *Vision Res.* **49,** 615–621
78. Bishop, C. E., Whitworth, D. J., Qin, Y., Agoulnik, A. I., Agoulnik, I. U., Harrison, W. R., Behringer, R. R., and Overbeek, P. A. (2000) *Nat. Genet.* **26,** 490–494
79. Qin, Y., Kong, L. K., Poirier, C., Truong, C., Overbeek, P. A., and Bishop, C. E. (2004) *Hum. Mol. Genet.* **13,** 1213–1218
80. Le, Y. Z., Zheng, W., Rao, P. C., Zheng, L., Anderson, R. E., Esumi, N., Zack, D. J., and Zhu, M. (2008) *Invest. Ophthalmol. Vis. Sci.* **49,** 1248–1253